

FCC catalyst attrition behavior at high temperatures

Saba Foroutan Ghazvini¹, Ali Afshar Ebrahimi¹, Seyed Hadi Jafarnia²

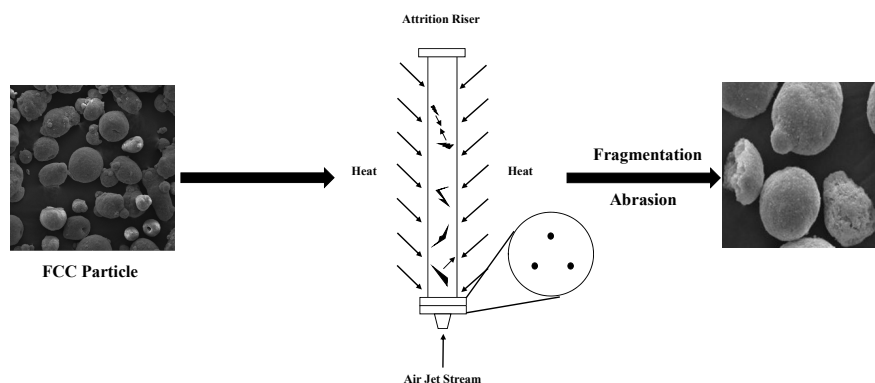
¹ Faculty of Petrochemicals, Iran Polymer and Petrochemical Institute, Tehran, Iran

² RFCC Senior Process Engineer, Process Engineering Department, Arak Oil Refinery, Arak, Iran

HIGHLIGHTS

- High temperature attrition tests which mimic the regenerator condition has been carried out on a FCC catalyst.
- Considerable reshaping of PSD plots reported extreme particles cracking at high temperature.
- Attrition process contour plots addressed optimization point and interaction between temperature and time.

GRAPHICAL ABSTRACT



ARTICLE INFO

Article history:

Received 12 October 2019

Revised 08 December 2019

Accepted 10 December 2019

Keywords:

FCC catalyst particles

Attrition

High temperature

RSM

PSD

ABSTRACT

In this work, high temperature attrition was studied in a standard attrition set-up to mimic the FCC regenerator environment with mechanical attrition. Operating conditions were modified in this pilot due to the application of high temperatures. Two parameters, i.e., time and temperature in the ranges of 1 to 5h and 673-973K, were surveyed, respectively. The behavior of attrition and mass loss was then modeled and validated. At higher temperatures mass loss response sensitivity became larger. Finally, PSD and SEM tests were used to investigate the attrition mechanism. In the ambient tests, abrasion was significant while at higher temperatures, fragmentation was considerable. PSD plots shifted into larger particles and SEM images showed those changes as well. In addition, significant reshaping in the PSD curves indicated particle cracking at high temperatures.

1. Introduction

A gas-solid fluidized bed reactor is the key item in the fluid catalytic cracking (FCC) process. FCC operates at high temperature and utilizes solid catalyst particles. Attrition is an indispensable problem in reactor fluidization and circulation in the unit. Gas-solid fluidized reactors are the core of industrial, chemical, and petrochemical processes due to the advantages of their good phases contact area, rapid mixing, and highly efficient transport phenomena [1-2]. Solid particle attrition is a crucial issue that refers to the process of particle resurfacing, reshaping, and size reduction [3]. The study of the attrition process has been done on many diverse materials such as: residue fluid cracking catalysts, methanol to olefin catalysts, and CO₂ adsorbents [4-7]. Particle attrition in fluidized bed reactors is very complicated and causes the abrasion and fragmentation mechanisms [8-9]. It is affected by various parameters of catalyst properties such as: morphology, cracks and synthetic compositions, feedstock contaminations and the engineering operational parameters such as temperature, pressure, and gas phase velocity [10].

Many studies have been done on the attrition behavior of diverse particle materials at ambient temperature such as crystals, like sodium chloride and sodium carbonate monohydrate particles, which are used in bulk chemical and detergent industries [11-13], coal ash particles used in combustion technology [14-15], iron Fischer-Tropsch catalyst used in slurry bubble column reactors (SBCR) or stirred tank slurry reactors (STSR) [16-19], glass [20], and oxygen carriers used in chemical looping combustion technology [21-23].

Scala *et al.* investigated limestone attrition at high temperature. The experiments were done in a stainless steel (AISI 312) fluidized bed reactor of 1m height and 40mm internal diameter. The reactor, which was filled with 100-200 gr samples, was heated up to 1123K before each batch run [24]. Lin *et al.* worked on the effect of high temperature and combustion conditions on silica sand attrition. The stainless steel (AISI 310) fluidized reactor was constructed with a 0.5m length preheating section connected to a main column with a height and internal diameter of 1 and 0.09m, respectively. The tests were done under an atmospheric pressure and temperature of 873, 973, and 1073K. The reported results showed that the attrition rate was higher at high temperatures and combustion conditions due to

the influence of thermal shock [25]. Lin *et al.* continued their previous study and proposed the attrition rate model at high temperature. The applied operating factors were a temperature, particle size, fluidized static bed height and velocity of the jet gas of 298-1173K, 385-1095 μ m, 1.2-2.0 H/D and 0.14-0.29 m/s, respectively [26]. Chen *et al.* assessed limestone particles attrition by utilization of impact tests at temperatures of 298-853K. The experiments were undertaken in the circulating system of a fluidized bed chamber. The system was comprised of a compressor, three-stage preheater, super heater, and an accelerating tubular combustor with a 1m length and 0.012 m internal diameter. They proposed two experimental correlations and stated the decrement of attrition by increasing the temperature [27]. They expanded their attrition research temperature to 1123K. Rittinger's surface theory analysis was employed [28], and the results stated that the attrition rate was affected by calcination and sulfation at 1123K; whereas, no effect was observed at less than 853K. The highest rate was for attrited calcined limestone at 1123K [29]. In continues process studies, the particle population model was proposed using the Arrhenius format [30]. Li *et al.* investigated the attrition behavior of the fluid coking process with supersonic convergent-divergent nozzles. The apparatus consisted of a high temperature fluidized reactor with 1.23m height and 0.1m \times 0.5m cross section. The attrition gas/gases were injected from the sidewall nozzles and tests were done from ambient temperature up to 773K. The obtained data revealed that the temperature had considerable effect on grinding efficiency, and Ghadiri's breakage model was applied to represent the effect. Moreover, fragmentation was the dominant mechanism in the hot attrition process [31]. Hartman *et al.* developed a high temperature attrition module for Lanov dolomite in catalytic biomass gasification. Experimental tests were conducted in a hot turbulent fluidized reactor with a 0.5m height, 0.051m inner diameter, and constant temperature of 1123K [32]. Recently, Hao *et al.* performed a high temperature attrition study for the MTO catalyst from 373-773K. A jet cup attrition apparatus was utilized and the breakthrough results offered the significant influence of gas velocity. Due to the transition of the attrition mechanism, the maximum attrition index was switched from 573 to 373K at the highest gas velocity [5].

Extensive study has been done on FCC catalysts attrition since 1949 [33]. The catalytic cracking process operates at high temperature and there are very few studies devoted to high temperature FCC catalyst attrition. The aim of this work is to investigate the FCC catalyst attrition behavior in high temperatures to mimic the regenerator conditions for the catalyst. Two operating attrition factors, i.e., time, 1-5h, and temperature, 673-973K, were chosen as A and B parameters, respectively. Statistical response surface methodology (RSM) with central composite design (CCD) was utilized to give us the layout of experimental tests and reveal the simultaneous interactive effect of attrition time and temperature. This study can predict the catalyst behavior in large scale FCC operation. Furthermore, the mathematical fundamentals of this method give accurate and reliable results. The generated contour plots, results of RSM, were in close agreement with numerical model rates. Finally, PSD and SEM analysis offered the dominant attrition mechanism in different operating conditions. Attrition of FCC catalyst particles at elevated temperatures has been very rarely studied, to the best of the author's knowledge.

2. Experimental Study

2.1. Attrition apparatus

Fig. 1 shows the schematic attrition system used in this work. The system was constructed at the Iran Polymer and Petrochemical Institute, IPPI, according to the procedures and sizing scales reported in ASTM-D-5757-00 [34]. The compressed air is the fluidizing agent in this apparatus. Due to the electrostatic forces of the generated fine particles, there is mitigation of solid particles. Therefore, the compressed air passes through 0.25m of deionized water. The size and structure of the deionized water column was extracted from the standard ASTM test method to reach the desired humidity. Pressurized air with the humidity of 30-40% flowed into the bottom of the attrition column through a distributor plate. The plate has three 0.0003m diameter nozzles arranged as a triangle 0.010m from the center of the triangle. According to the standard, the inlet flowrate was controlled so that the outlet flowrate became 10 L/h in each test. The attrition column consisted of an attrition riser and a settlement chamber. The attrition riser, with 0.710m height and

0.035m internal diameter, was made of stainless steel (AISI 310). This research was designed to assess high-temperature experimental tests; therefore, a specific furnace was constructed for the attrition riser section. The riser section was located in a 4.4kW electrical furnace for high-temperature tests. In each run, the riser was filled with 50g catalyst sample according to the ASTM test. The riser connects to the 0.630m settlement chamber. The first conical part expands to a 0.110m internal diameter, which was welded to 0.300m height tubular column. Finally, a convergent conical shape was abridged to 0.030m diameter and lined to the fines collector bag. The collector is a vertical cylindrical chamber whose bottom is a classic general purpose filter paper. So, the fine particles entrained from the riser were properly collected above the filter.

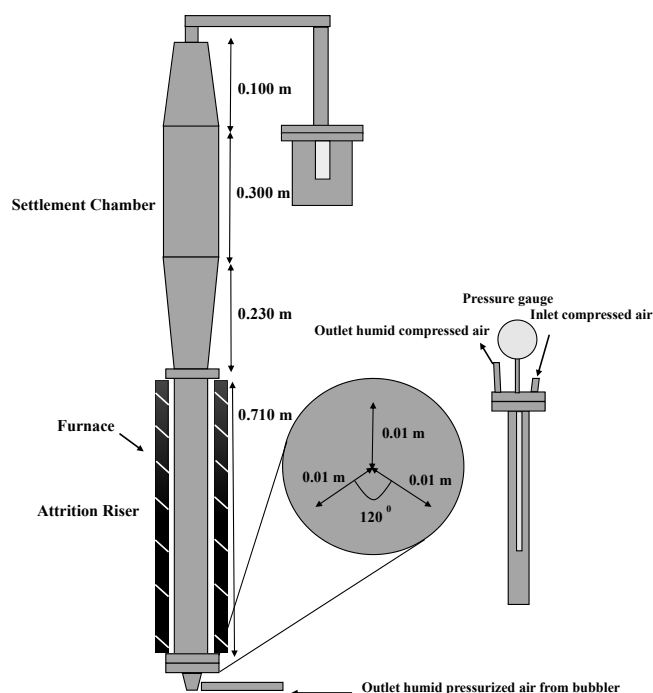


Fig. 1. Attrition system schematic.

2.2. Catalyst characterization tests

A fresh catalyst sample was provided from a domestic refinery. Catalyst properties, such as bulk density and particle density, were measured and the BET surface area of the catalyst was calculated using a CHEMBET-3000 analyzer. Table 1 reports the properties results. For further study of the impacts of operational conditions, morphology and surface structure were observed with a VEGA II TESCAN scanning electron microscope. SEM tests were done on catalyst samples before and after the tests. Particle size distribution was also one of

Table 1. Properties of fresh catalyst sample.

Bulk density (g/ml)	Particle density (g/ml)	Specific surface area (m ² /g)
0.80	2.17	208.410

the most important analyses which shows the dominant mechanism or mechanism transfer at different processing conditions. PSD graphs were generated after 1h and 5h tests for ambient temperature, 673K, and 973K with Malvern Mastersizer 2000. Those PSD results were done for the remaining catalyst over the jet nozzles plate.

2.3. Experiments layout

Processing conditions impacts and relevant mechanisms were inferred from the generated fine mass in the downstream of the set-up. Response Surface Methodology is a combination of mathematics and statistical techniques for monitoring and analyzing a process. It is utilized in engineering for optimization of multi-factorial operating conditions. Two factors, i.e., time and temperature, were chosen and entitled as A and B, respectively. Temperature is the most imperative feature of FCC reactor processing. Time is another significant parameter because the FCC catalyst is being circulated in the unit for long time periods. Therefore, these two parameters were selected to mimic the closest points of industrial conditions and to report challenges. "A" ranges from 1 to 5h and "B" ranges from 673 to 973K. These data were imported to the Design Expert calculation tool (DX 7.0.0) for processing. The experiments layouts were generated with the central composite design. Table 2 reports the related factors, units and ranges. The response of the experimental design is the collected mass loss of fine particles in grams. In each run, the weight of the collector before and after the test was measured with a digital scale. The difference shows the mass of collected attrition loss. Then, the mass loss was removed, and the collector was weighed again to ensure the validity and exactness of the measured mass.

Table 2. Design of experimental runs with central composite design (CCD).

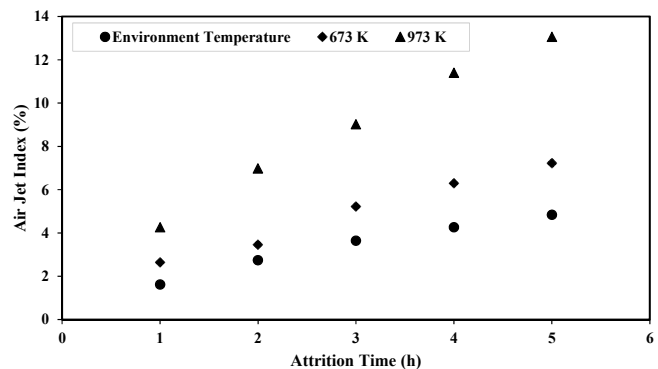
Factors	Symbol	Unit	Level (Coded and Real)		
			-1	0	1
Attrition time	A	h	1	3	5
Temperature	B	K	673	823	973

3. Results and Discussion

3.1. Air jet index

ASTM-D-5757-00 offered a dimensionless numerical value entitled the Air Jet Index (AJI). The AJI refers to the percentage of catalyst loss in attrition processing 5h following equation 1. AJI gives a better estimated vision for the attrition resistance of a catalyst used on the industrial scale. Jones *et al.* developed this index for longer time ranges and to compare the AJI transition for different catalysts [3]. In this study, the Air Jet Index was calculated and reported in Fig. 2. Numerical values were obtained over five-hour attrition in ambient temperature, 673K, and 973K. The test results demonstrated that the loss rate increases smoothly in moderate temperatures, such as 673K, and at higher temperatures, i.e., 973K, there was an intense transition due to thermal shock. So, temperature plays a significant role in the attrition tests, and the catalyst physical-thermal resistance underwent considerable changes.

$$AJI = \frac{\text{collected fine particles weight}}{\text{initial catalyst bed weight}} \times 100 \quad (1)$$

**Fig. 2.** Air jet index for attrition loss.

3.2. Statistical results

Experimental tests were done according to the DX (Design Expert) calculation tool results. A RSM package with a central composite design was selected from the DX calculation tool. The experimental test layout and the obtained results through 13 tests are reported in Table 3. It was observed that the highest fine particles loss occurred at 973K and 5h attrition, and this record was followed by 1035K-3h and 823K-5.83h in second and third places, respectively. The top three

Table 3. Experimental layouts of catalyst mass loss.

Run no.	Calculated information				Calculated results
	A		B		Down-stream mass distribution (g)
	Attrition time (h)		Temperature (K)		
Coded value	Real value	Coded value	Real value	Real value	
1	1.000	5.00	1.000	973.00	6.55
2	1.000	5.00	-1.000	673.00	3.61
3	0.000	3.00	-1.414	610.87	2.82
4	0.000	3.00	0.000	823.00	4.06
5	0.000	3.00	1.414	1005.13	4.81
6	0.000	3.00	0.000	823.00	4.06
7	-1.000	1.00	-1.000	673.00	1.58
8	-1.414	0.17	0.000	823.00	0.76
9	0.000	3.00	0.000	823.00	4.00
10	1.414	5.83	0.000	823.00	4.57
11	0.000	3.00	0.000	823.00	4.06
12	-1.000	1.00	1.000	973.00	2.29
13	0.000	3.00	0.000	823.00	4.00

experimental catalyst loss in Table 3 defines the two parameters interaction along with the optimized point. DX design considers the result of tests slightly more than the upper limit and lower than the minimum limit to certify there are no sharp changes over the operating parameters-slot. Therefore, two tests at 5.83 and 0.17h were performed.

3.3. ANOVA results

The DX calculation tool utilizes analysis of variance program (ANOVA) for the regression of results, which

were obtained from experimental tests. This analysis program proposes the best fitted polynomial model and multifactorial contour plots. The coefficients of the model represent the effect of each operating factors and interaction influences. In the ANOVA program, the validity of the results are measured with statistical F-value and P-value, and the reliability of the proposed model is assessed with R^2 and adj. R^2 . ANOVA results are reported in Table 4. The P-value for the sample catalyst is <0.0001 , which is less than the 0.05 target. Therefore, the fitted model is significant and accurate. R^2 and adj. R^2 are 0.9936 and 0.9891, respectively. These values are

Table 4. Catalyst mass loss via ANOVA results.

Source	Sum of squares	df	Mean of squares	F-Value	P-Value (Prob. >F)	Significance
Model	8.613E-003	5	1.723E-003	218.81	<0.0001	Significant
A	5.757E-003	1	5.755E-003	731.27	<0.0001	
B	1.307E-003	1	1.307E-003	166.04	<0.0001	
AB	1.488E-004	1	1.488E-004	18.91	0.0034	
A ²	1.398E-003	1	1.398E-003	177.59	<0.0001	
B ²	1.257E-005	1	1.257E-005	1.60	0.2469	
Residual	5.511E-005	7	7.873E-006			
Cor Total	0.75	12				

Standard Deviation =2.806E-003
Mean =0.33
Coefficient of Variation (C.V.%) = 0.86
Predicted Residual Error of Sum of Squares (PRESS) = 3.816E-004

$R^2 = 0.9936$
Adj $R^2 = 0.9891$
Pred $R^2 = 0.9560$
Adeq Precision = 50.613

Table 5. Generated model for catalyst mass loss (in g).

Response Surface Linear Model (A and B are coded values)

$$\frac{1}{\text{Sqrt}(\text{Downstreammassloss} + 6)} = 0.32 - 0.027A - 0.013B - (6.100E - 003)AB + 0.014A^2 + (1.344E - 003)B^2$$

Response Surface Linear Model (Time and temperature with actual values)

$$\frac{1}{\text{Sqrt}(\text{Downstreammassloss} + 6)} = 0.41906 - 0.023495(\text{Time}) - (8.9924E - 005)(\text{Temperature}) - (2.03333E - 005)(\text{Time} \times \text{Temperature}) + (3.54421E - 003)(\text{Time})^2 + (5.97327E - 008)(\text{Temperature})^2$$

close to 1, which demonstrates the model fits well with the experimental data. The generated models are shown in Table 5 with actual and coded values.

3.4. Optimization plots analysis

2D and 3D operation contour plots were obtained from simultaneous statistical equation solving and data regression, which are reported in Fig. 3. At initial attrition time, temperature played the dominant role. As the test time increased, the slope of the contour lines

decreased. This shows the synergic impact of time on the attrition loss. The minimum mass loss condition was 973K and 1h, which is followed by 610.87K-3h. The interaction term was mostly significant at higher processing times.

3.5. Characterization tests analysis

Particle size distribution graphs at ambient temperature, 673 and 973K for 1 and 5h attrition times are reported in Figs. 4 and 5. The largest particles size in the PSD plot in Fig. 4 were nearly 240µm, while those in Figure 5 were about 200µm. These show the breakage of the particles and changes in the PSD curve area. At the start of the test, fine particles from the initial samples migrated and were collected in the filter bag. Therefore, it was observed that the PSD peak shifted slightly to the right. The vertical axis is the volume percentage. Since the migration of generated and original fine particles occurs during attrition, the remaining catalyst on the orifice has more larger particles. So, the shift of PSD lines to the right was observed. In the high temperature tests, the curves peak switched smoothly to the left from the 1 to 5h run. This represents the abrasion of catalysts particles due to more attrition time, and implies new fine particles were generated from the parent particles. This proves that as time increases abrasion plays a more important role. As the temperature increases, fragmentation will become more significant in attrition. Width changes of the curves was another important factor of the PSD curve at different operating temperatures. With the abrasion mechanism, the PSD lines smoothly shift right-left and up-down directions without considerable change. But with the fragmentation mechanism, the width has been changed. It is also observed that this transition is considerably more at 973K. This shows that the thermal shock had

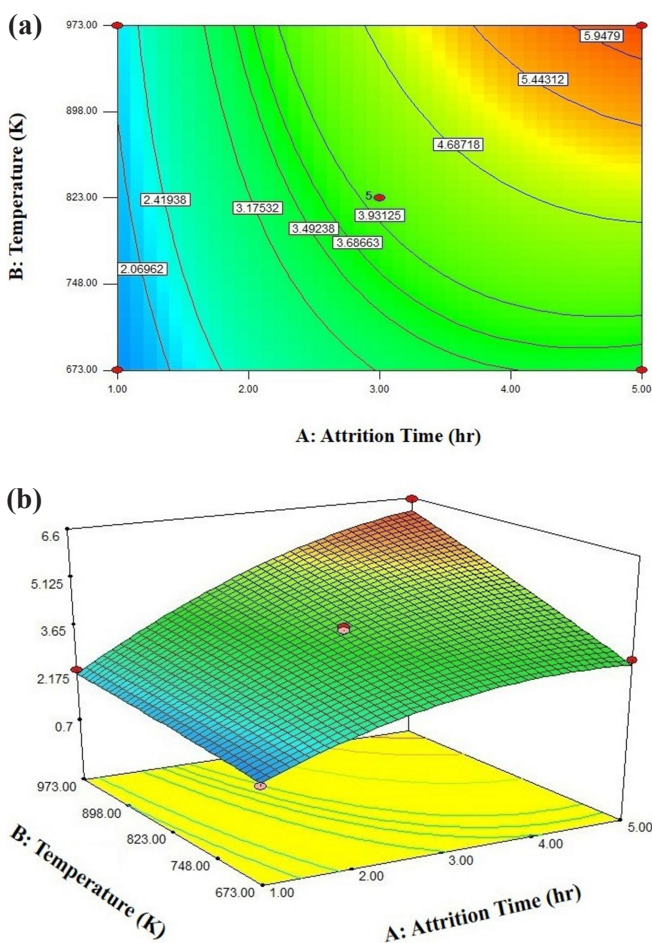


Fig. 3. Operation contour plots (a) 2 dimensional and (b) 3 dimensional.

an impact on fragmentation, and it is more significant at higher temperatures. So, fragmentation is the dominant mechanism of attrition in this condition. Therefore, when these two parameters are working together, the attrition condition is complicated and perceiving the dominant mechanism is challenging. Therefore, statistical-mathematical methods, like RSM, are useful for better understanding of the process. It also helps to have a better visualization for higher temperatures similar to industrial conditions. Part “a” in Fig. 6 is the SEM images of a fresh sample, and part “b” is the SEM of the attrited catalyst at a constant temperature of 973K for 5h. It is observed from part b that the small size particles produced from cracking, thermal, and physical shocks have left the system. These image results support the peak shifts of the PSD plots to the right.

4. Conclusion

FCC catalyst attrition tests were done according to ASTM-D-5757-00. Regarding the operation of FCC process at high temperature, the attrition pilot was

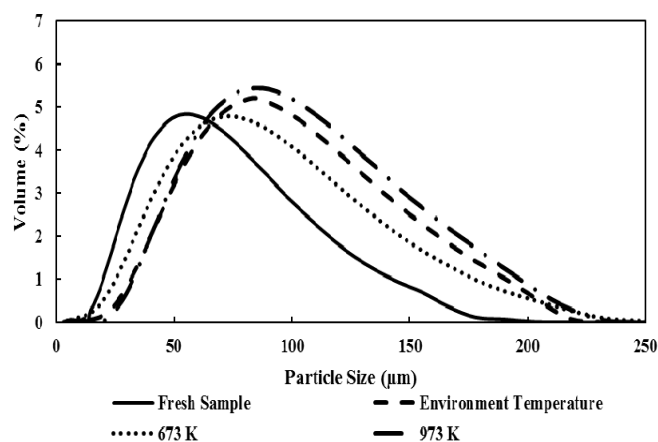


Fig. 4. Particle size distribution for 1h operating time.

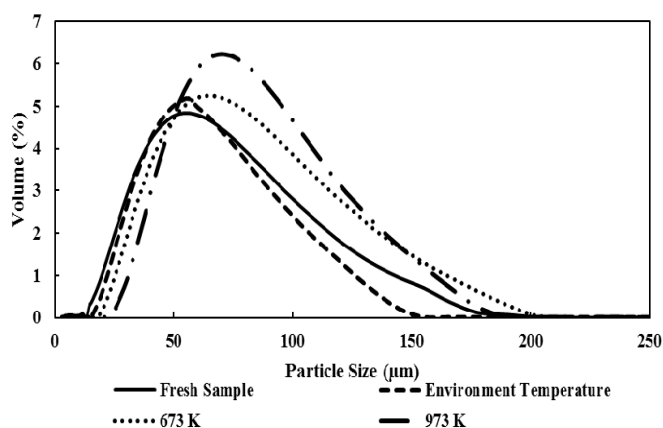


Fig. 5. Particle size distribution for 5h operating time.

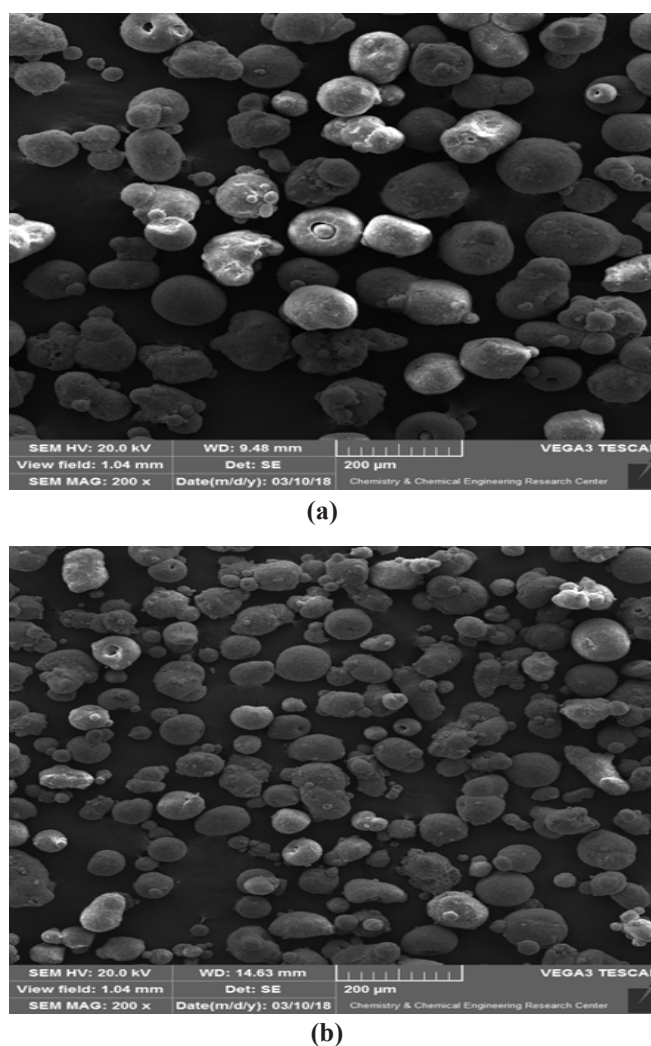


Fig. 6. SEM images of (a) fresh sample and (b) attrited catalyst.

facilitated with a 4.4kW furnace. Two operational parameters, i.e., time and temperature in the range of 1-5h and 673-973K, were selected, respectively. Response surface methodology with a central composite design was utilized for the investigation of individual parameters' impact and interaction influences. According to the experimental results regression, the best fitted model was proposed and operating contour plots were generated. At early attrition times, especially before the second hour, although temperature was the affecting parameter on the mass loss with abrasion mechanism, it showed a synergic effect at higher temperatures and made the mass loss response more sensitive to temperature, which resulted in fragmentation. Moreover, PSD plot peaks moved toward larger particle sizes after the test and considerable shape changes especially at 973K/5h were observed from 1 to 5h run. Shape change confirms that fragmentation is the key mechanism of attrition due to thermal shock impact. At this point, it is perceived that not only physical resistance but also thermal resistance

is of great significance. SEM images supported those results and reported larger size particles. At higher temperatures, smaller particles generated from the initial hours undergo multi-fragmentation and migrated from the system, bigger particle sizes settled down in the riser and were recognized in the SEM image. This study mimicked the regenerator section of a FCC, where physical attrition of the catalyst particles in the presence of high temperature takes place. So the results of this study can help catalyst manufacturers to consider some measurements against the thermal shock effect on the physical attrition of the particles. Study of the attrition riser hydrodynamic at different temperatures is suggested for future study.

References

- [1] F. Scala, R. Chirone, P. Salatino, in: F. Scala (Ed.), *Fluidized bed technologies for near-zero emission combustion and gasification*, Woodhead Publishing Limited, New York (2013).
- [2] J. Werther, J. Reppenhagen, in: W.C. Yang (Ed.), *Handbook of fluidization and fluid-particle systems*, Marcel Dekker, New York (2003).
- [3] T.J. Jones, J.K. Russel, C.J. Lim, N. Ellis, J.R. Grace, Pumice attrition in an air jet, *Powder Technol.* 308 (2017) 298-305.
- [4] W.L. Forsythe, W.R. Hertwig, Attrition characteristics of fluid cracking catalysts-laboratory studies, *J. Ind. Chem. Res.* 41 (1949) 1200-1206.
- [5] J. Hao, Y. Zhao, M. Ye, Z. Liu, Attrition of methanol to olefins catalyst in jet cup, *Powder Technol.* 316 (2017) 79-86.
- [6] A. Knight, N. Ellis, J.R. Grace, C.J. Lim, CO₂ sorbent attrition testing for fluidized bed systems, *Powder Technol.* 266 (2014) 412-423.
- [7] Z. Sun, M. Xiao, S. Wang, D. Han, S. Song, G. Chenb, Y. Meng, Electrostatic shield effect: an effective way to suppress dissolution of polysulfide anions in lithium-sulfur battery, *J. Mater. Chem.* 2 (2014) 15938-15944.
- [8] B. Ambelard, S. Bertholin, C. Bobin, T. Gauthier, Development of an attrition evaluation method using a Jet Cup rig, *Powder Technol.* 274 (2015) 455-465.
- [9] Y.C. Ray, T.S. Jiang, C.Y. Wen, Particle attrition phenomena in a fluidized bed, *Powder Technol.* 100 (1998) 193-206.
- [10] C.R. Bemrose, J. Bridgewater, A review of attrition and attrition test methods, *Powder Technol.* 49 (1987) 97-126
- [11] K.R. Yuregir, M. Ghadiri, R. Clift, Impact attrition of sodium chloride crystals, *Chem. Eng. Sci.* 42 (1987) 843-853.
- [12] M. Ghadiri, K.R. Yuregir, H.M. Pollock, J.D.J. Ross, N. Rolfe, Influence of processing conditions on attrition of NaCl crystals, *Powder Technol.* 65 (1991) 311-320.
- [13] J.A.S. Cleaver, M. Ghadiri, Impact attrition of sodium carbonate monohydrate crystals, *Powder Technol.* 76 (1993) 15-22.
- [14] J.J. Pis, A. B. Fuertes, V. Artos, A. Suarez, F. Rubiera, Attrition of coal ash in a fluidized bed, *Powder Technol.* 66 (1991) 41-46.
- [15] J. Tomeczek, P. Mocek, Attrition of coal ash particles in a fluidized-bed reactor, *AIChE J.* 53 (2007) 1159-1163.
- [16] D.S. Kalakkad, M.D. Shroff, S. Köhler, N. Jackson, A.K. Datye, Attrition of precipitated iron Fischer-Tropsch catalysts, *Appl. Catal. A*, 133 (1995) 335-350.
- [17] R. Zhao, J.G. Goodwin Jr., K. Juthimurugesan, S. K. Gangwal, J.J. Spivey, Spray-dried iron Fischer-Tropsch catalyst. 1. Effect of structure on the attrition resistance of the catalysts in the calcined state, *Ind. Eng. Chem. Res.* 40 (2001) 1065-1075.
- [18] R. Zhao, J.G. Goodwin Jr., K. Juthimurugesan, S. K. Gangwal, J.J. Spivey, Spray-dried iron Fischer-Tropsch catalyst. 2. Effect of carbonization on catalyst attrition resistance, *Ind. Eng. Chem. Res.* 40 (2001) 1320-1328.
- [19] T.J. Lin, X. Meng, L. Shi, Attrition studies of an iron Fischer-Tropsch catalyst used in a pilot-scale stirred tank slurry reactor, *Ind. Eng. Chem. Res.* 51 (2012) 13123-13131.
- [20] M. Stein, J.P.K. Seville, D.J. Parker, Attrition of porous glass particles in a fluidized bed, *Powder Technol.* 100 (1998) 242-250.
- [21] L. Guo, H.B. Zhao, J.C. Ma, D.F. Mei, C.G. Zheng, Comparison of large-scale production methods of Fe₂O₃/Al₂O₃ oxygen carriers for chemical looping combustion, *Chem. Eng. Technol.* 37 (2014) 1211-1219.
- [22] M. Arjmand, V. Frick, M. Ryden, H. Leion, T.P. Mattisson, A. Lyngfelt, *Energ. Fuel.* 29 (2015) 1868-1880.
- [23] G. Azimi, T. Mattison, H. Leion, M. Ryden, A.

- Lyngfeld, Comprehensive study of Mn-Fe-Al oxygen-carriers for chemical-looping with oxygen uncoupling (CLOU), *Int. Greenh. Gas Con.* 34 (2015) 12-24.
- [24] F. Scala, A. Cammarota, R. Chironne, P. Salatino, Comminution of limestone during batch fluidized-bed calcination and sulfation, *AIChE J.* 43 (1997) 363-373.
- [25] C.L. Lin, M.Y. Wey, Effects of high temperature and combustion on fluidized material attrition in a fluidized bed, *Korean J. Chem. Eng.* 20 (2003) 1123-1130.
- [26] C.L. Lin, M.Y. Wey, Influence of hydrodynamic parameters on particle attrition during fluidization at high temperature, *Korean J. Chem. Eng.* 22 (2005) 154-160.
- [27] Z. Chen, C.J. Lim, J.R. Grace, Study of limestone particle impact attrition, *Chem. Eng. Sci.* 62 (2007) 867-877.
- [28] Y.C. Ray, T.S. Jiang, T.L. Jiang, Particle population model for a fluidized bed with attrition, *Powder Technol.* 52 (1987) 35-48.
- [29] Z. Chen, J.R. Grace, C.J. Lim, Limestone particle attrition and size distribution in a small circulating fluidized bed, *Fuel*, 87 (2008) 1360-1371.
- [30] Z. Chen, J.R. Grace, C.J. Lim, Development of particle size distribution during limestone impact attrition, *Powder Technol.* 207 (2011) 55-64.
- [31] F. Li, C. Briens, F. Berruti, J. McMillan, Particle attrition with supersonic nozzles in a fluidized bed at high temperature, *Powder Technol.* 228 (2012) 285-294.
- [32] M. Hartman, K. Svoboda, M. Pohorely, M. Syc, M. Jeremias, Attrition of dolomitic lime in a fluidized-bed reactor at high temperature, *Chem. Pap.* 67 (2013) 164-172.
- [33] W.L. Forsythe, W.R. Hertwig, Attrition characteristics of fluid cracking catalysts. Laboratory studies, *Ind. Eng. Chem.* 41 (1949) 1200-1206.
- [34] ASTM-D-5757-00, Standard test method for determination of attrition and abrasion of powdered catalysts by air jet, ASTM (2006).